

Supporting information

Ultrathin two-dimensional cobalt-organic framework nanosheets for high-performance electrocatalytic oxygen evolution

Yuxia Xu,^a Bing Li,^a Shasha Zheng,^a Ping Wu,^a Jingyi Zhan,^a Huaiguo Xue,^a Qiang Xu,^{a,b} Huan Pang,*^a

^aSchool of Chemistry and Chemical Engineering, Institute for Innovative Materials and Energy, Yangzhou University, Yangzhou, 225009, Jiangsu, P. R. China.

^bNational Institute of Advanced Industrial Science and Technology, (AIST), Ikeda, Osaka 563-8577, Japan.

Table of Contents

Electrochemical measurement and calculation	S4
Figure S1. Low-magnification SEM image of ultrathin 2D Co-MOF nanosheets.	S5
Figure S2. SEM images of Co-MOFs. (a,b) micro-nano Co-MOFs. (c,d) bulk Co-MOFs.	S6
Figure S3. (a,b) Low-voltage TEM images of ultrathin 2D Co-MOF nanosheets at different magnifications.	S7
Figure S4. EDX spectrum of ultrathin 2D Co-MOF nanosheets, and the inserted table summarizes the weight and atomic ratios of elements in the ultrathin 2D Co-MOF nanosheets.	S8
Figure S5. AFM images of ultrathin 2D Co-MOF nanosheet. The inset is the corresponding thickness curves of a single sheet.	S9
Figure S6. PXRD patterns of the Co-MOF samples obtained at different preparation conditions.	S10
Figure S7. XPS survey spectra of the Co-MOF materials.	S11
Figure S8. FTIR spectra of ultrathin Co-MOF nanosheets and its micro-nano/bulk counterparts. All the characteristic peaks are similar for all the samples, indicating they have similar functional groups.	S12
Figure S9. The raw CV curve (no iR compensation) and the real CV curve (95% iR compensation) of ultrathin 2D Co-MOF nanosheets.	S13
Figure S10. The raw LSV curve (no iR compensation) and the real LSV curve (95% iR compensation) of ultrathin 2D Co-MOF nanosheets.	S14
Figure S11. Cyclic voltammograms of (a) ultrathin 2D Co-MOF nanosheet, (b) micro-nano Co-MOF and (c) bulk Co-MOF materials at scan rates from 5 to 100 mV s ⁻¹ . (d) Estimating the C _{dl} and relative electrochemically active surface areas.	S15

Figure S12. PXRD patterns of ultrathin 2D Co-MOF nanosheets before and after the OER test.	S16
Figure S13. SEM image of ultrathin 2D Co-MOF nanosheets after 12000 s OER test.	S17
Figure S14. SEM image of ultrathin 2D Co-MOF nanosheets after 20 h OER test.	S18
Figure S15. Co 2p XPS spectra of ultrathin 2D Co-MOF nanosheets before and after the OER (12000 s) test.	S19
Figure S16. Chronoamperometric plot ($J_0 = 10 \text{ mA cm}^{-2}$) of ultrathin 2D Co-MOF nanosheets at a static overpotential of 263 mV after the 20 h OER test.	S20
Figure S17. (a) N_2 adsorption-desorption isotherms, and (b) the corresponding BJH pore size distribution of the ultrathin 2D Co-MOF nanosheets (inset: image magnification of pore size distribution from 0 to 10 nm).	S21
Figure S18. Nyquist plots of the different Co-MOF samples at 1.493 V (vs the RHE).	S22
Table S1. Comparison of the OER activity for several recently reported highly active cobalt-based electrocatalysts and the $\text{Co}_2(\text{OH})_2\text{BDC}$ nanosheets.	S23
Table S2. Comparison of the OER catalytic performance of different MOFs.	S24

Electrochemical calculation

Through adjusting to the Tafel equation ($\eta = b \log j + a$, where η is the overpotential, b is the Tafel slope, j is the current density and a is the exchange current density), the Tafel slopes and exchange current densities could be calculated for Co-MOF. In addition, the transfer number per oxygen molecule involved in oxygen reduction can be determined by Koutecky-Levich equations: $1/j = 1/j_L + 1/j_K = 1/B\omega^{0.5} + 1/j_K$, $B = 0.62nFC_0(D_0)^{2/3}v^{1/6}$, $j_K = nFkC_0$, in which j represents the measured current density, j_L and j_K are the diffusion-limiting and kinetic current densities, ω is the angular velocity of the disk ($\omega = 2\pi N$, where N is the linear rotation speed), n is the overall number of electrons transferred in oxygen reduction, F is the Faraday constant ($F = 96485 \text{ C mol}^{-1}$), C_0 is the bulk concentration of O_2 ($C_0 = 1.1 \times 10^{-6} \text{ mol cm}^{-3}$), D_0 is the diffusion coefficient of O_2 ($D_0 = 1.9 \times 10^{-5} \text{ cm}^2 \text{ s}^{-1}$), v is the kinematic viscosity of the electrolyte ($v = 0.01 \text{ cm}^2 \text{ s}^{-1}$), and k is the electron transfer rate constant.^{1,2} The TOF value is calculated from the following equation: $\text{TOF} = jA/4Fm$, j is the current density at overpotential of 300 mV in A cm^{-2} , A is the area of the electrode, F is the Faraday constant of 96485 C mol^{-1} , m is the number of moles of the active materials that are deposited onto the GC.

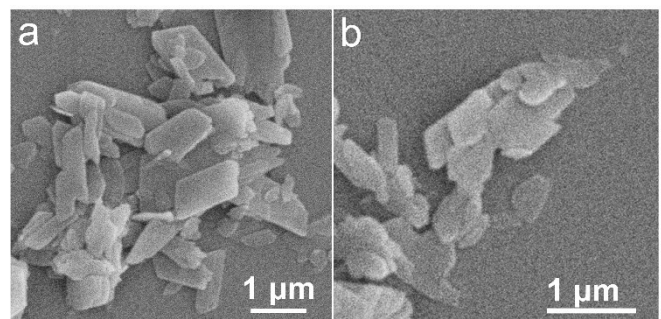


Figure S1. Low-magnification SEM image of ultrathin 2D Co-MOF nanosheets.

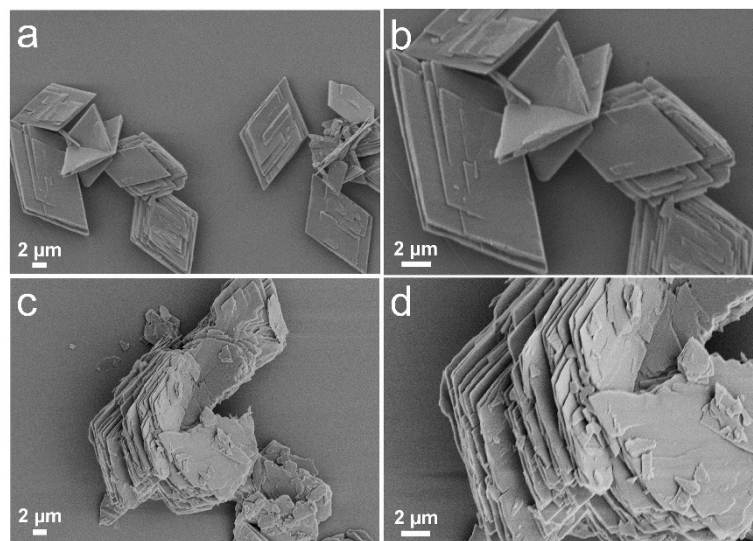


Figure S2. SEM images of Co-MOFs. (a,b) micro-nano Co-MOFs. (c,d) bulk Co-MOFs.

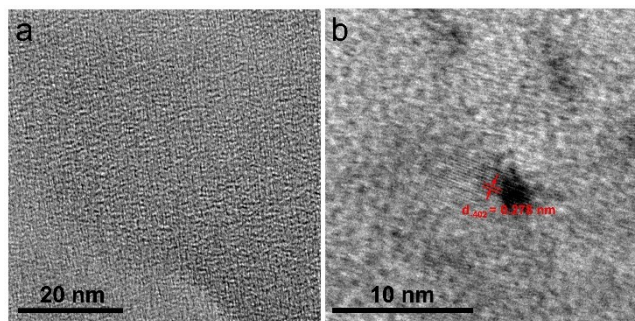


Figure S3. (a,b) Low-voltage TEM images of ultrathin 2D Co-MOF nanosheets at different magnifications.

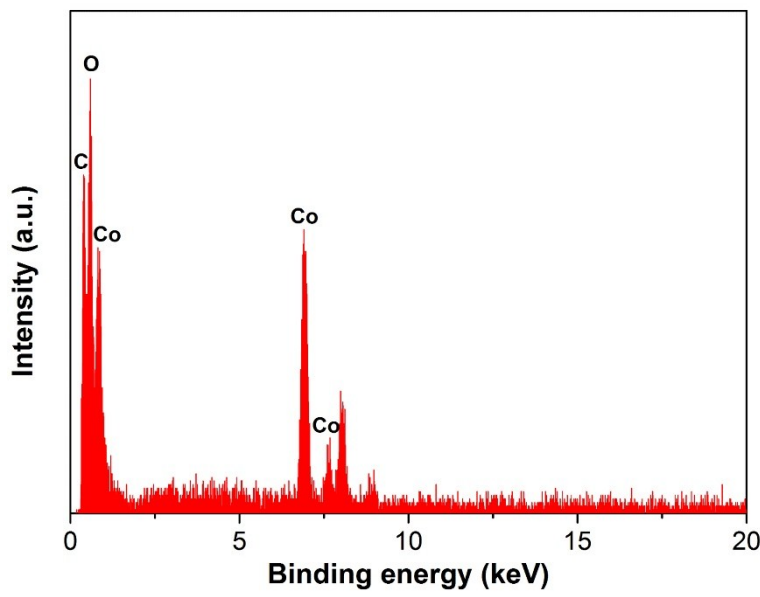


Figure S4. EDX spectrum of ultrathin 2D Co-MOF nanosheets, and the inserted table summarizes the weight and atomic ratios of elements in the ultrathin 2D Co-MOF nanosheets.

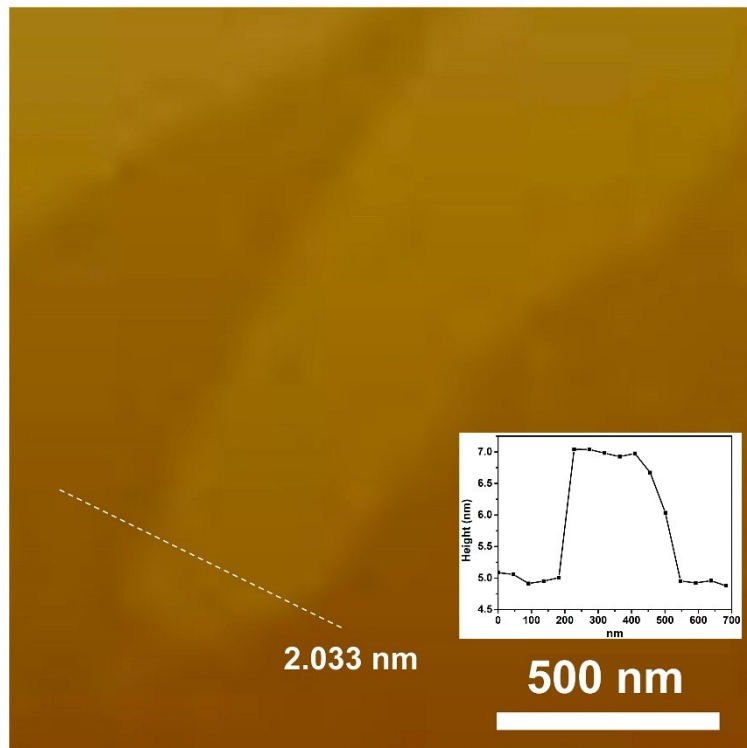


Figure S5. AFM image of ultrathin 2D Co-MOF nanosheet. The inset is the corresponding thickness curves of a single sheet.

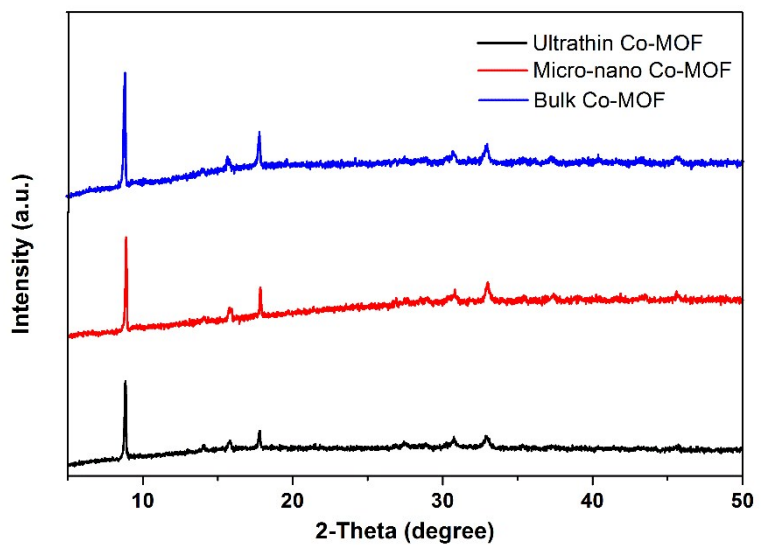


Figure S6. PXRD patterns of the Co-MOF samples obtained at different preparation conditions.

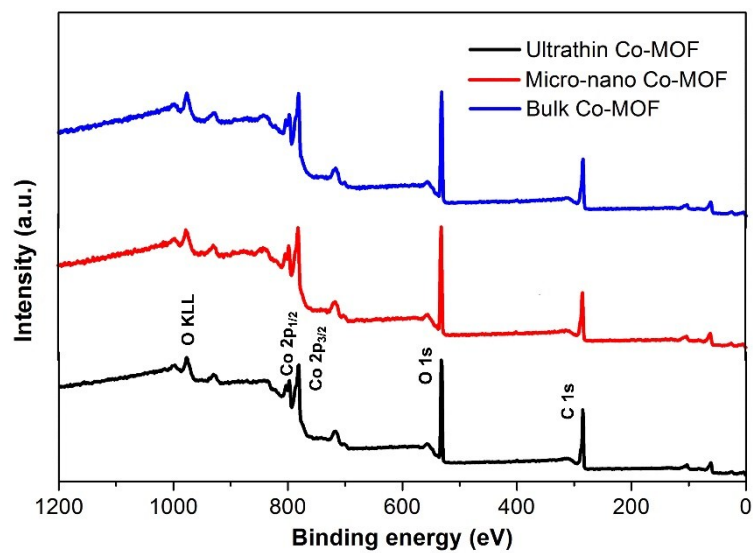


Figure S7. XPS survey spectra of the Co-MOF materials.

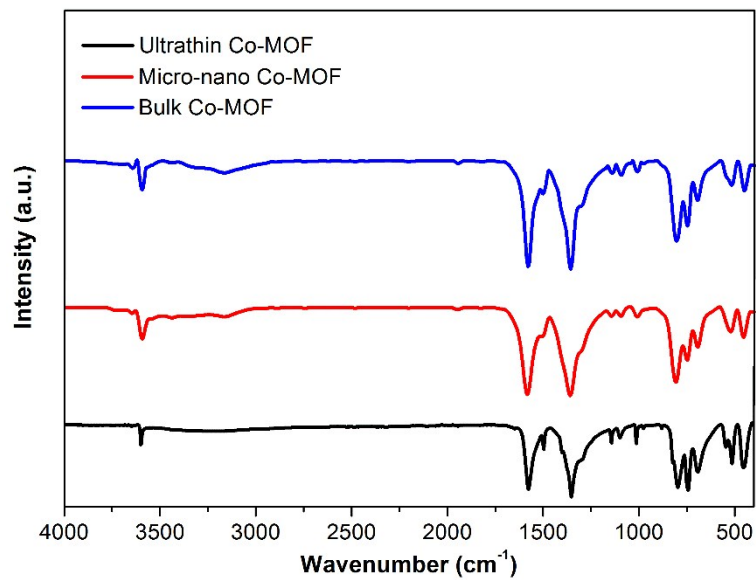


Figure S8. FTIR spectra of ultrathin Co-MOF nanosheets and its micro-nano/bulk counterparts.

All the characteristic peaks are similar for all the samples, indicating they have similar functional groups.

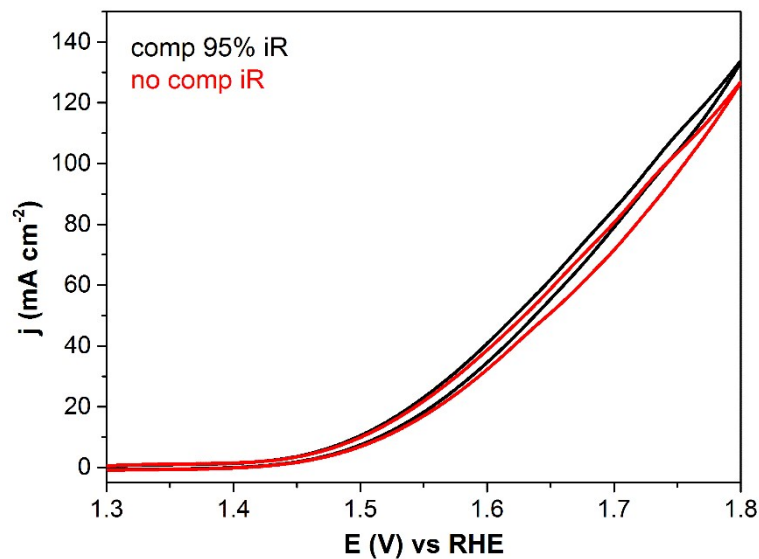


Figure S9. The raw CV curve (no iR compensation) and the real CV curve (95% iR compensation) of ultrathin 2D Co-MOF nanosheets.

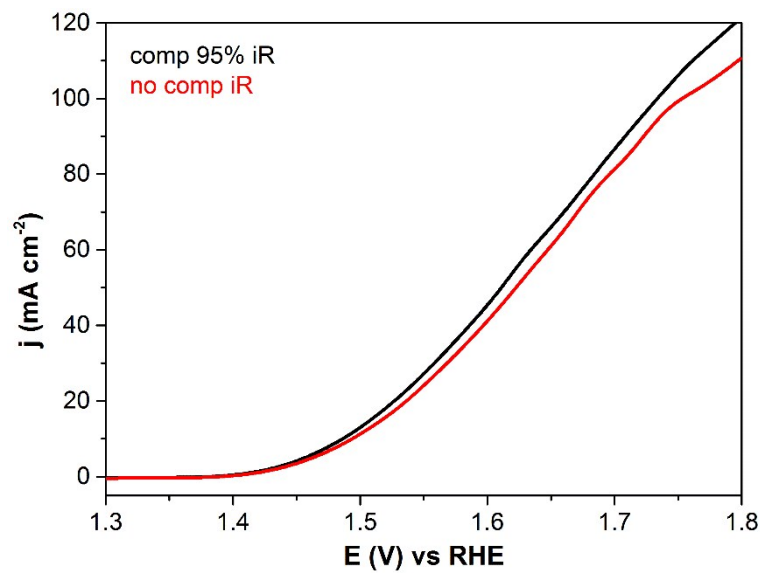


Figure S10. The raw LSV curve (no iR compensation) and the real LSV curve (95% iR compensation) of ultrathin 2D Co-MOF nanosheets.

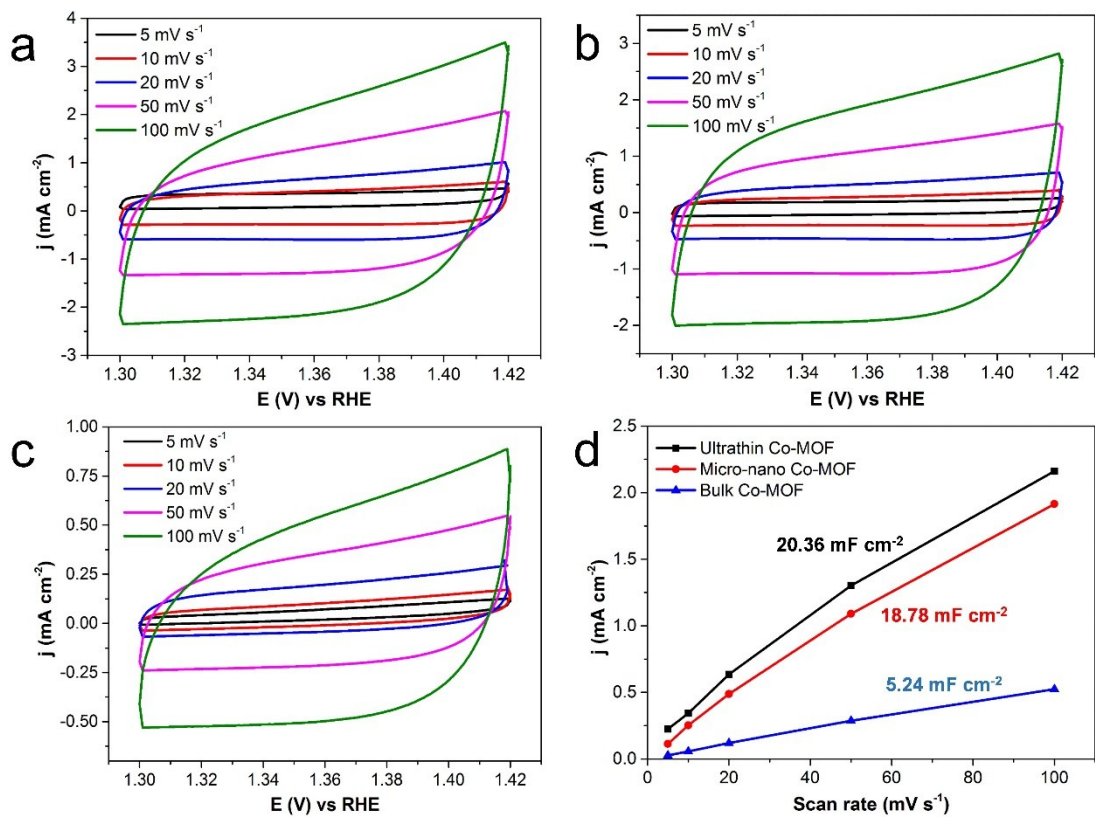


Figure S11. Cyclic voltammograms of (a) ultrathin 2D Co-MOF nanosheet, (b) micro-nano Co-MOF and (c) bulk Co-MOF materials at scan rates from 5 to 100 mV s^{-1} . (d) Estimating the C_{dl} and relative electrochemically active surface areas.

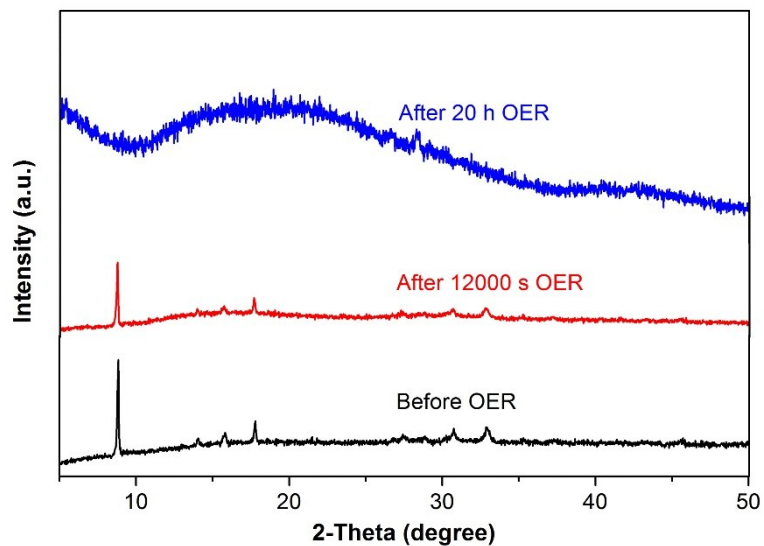


Figure S12. PXRD patterns of ultrathin 2D Co-MOF nanosheets before and after the OER test.

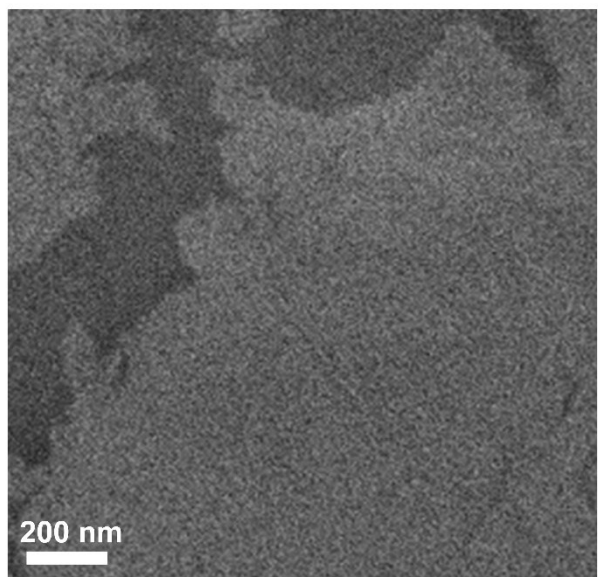


Figure S13. SEM image of ultrathin 2D Co-MOF nanosheets on electrode surface after 12000 s OER test.

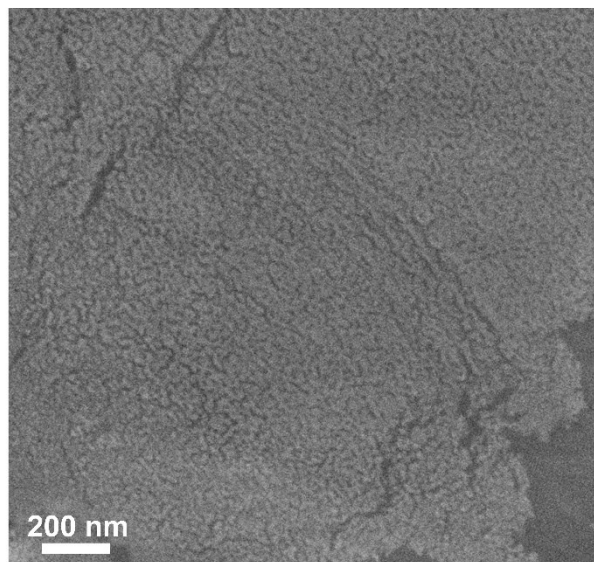


Figure S14. SEM image of ultrathin 2D Co-MOF nanosheets on electrode surface after 20 h OER test.

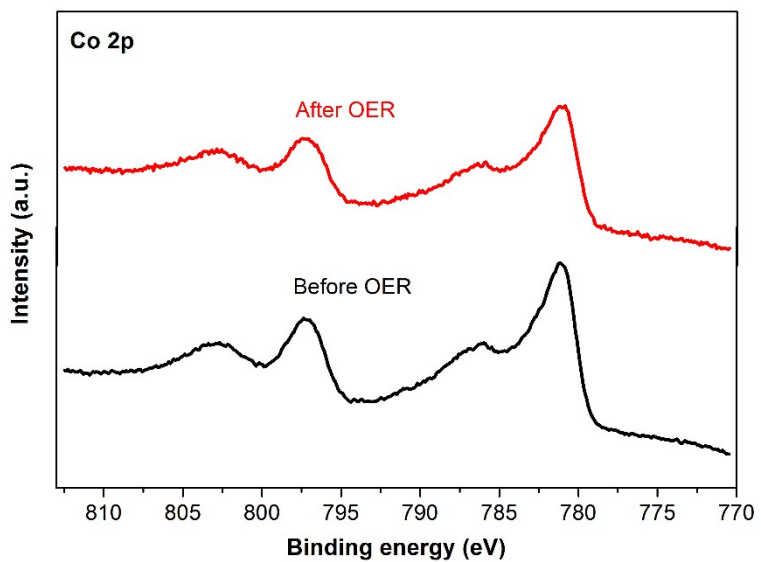


Figure S15. Co 2p XPS spectra of ultrathin 2D Co-MOF nanosheets before and after the OER (12000 s) test.

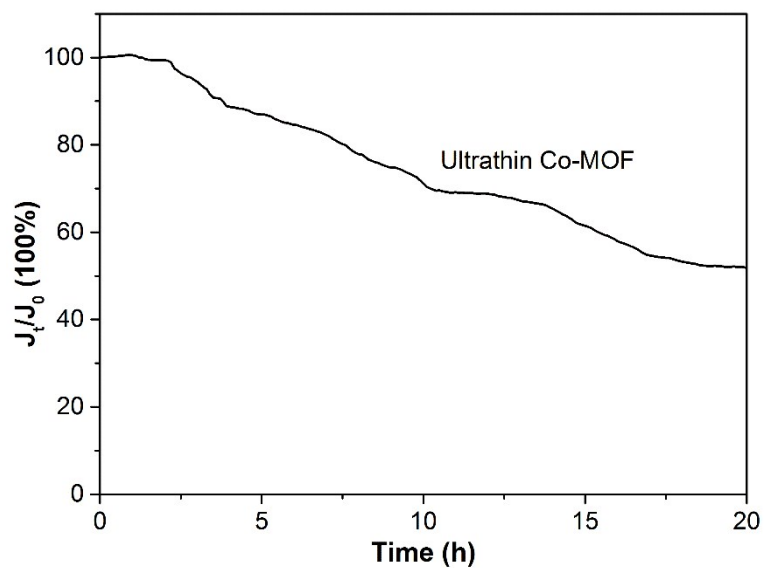


Figure S16. Chronoamperometric plot ($J_0 = 10 \text{ mA cm}^{-2}$) of ultrathin 2D Co-MOF nanosheets at a static overpotential of 263 mV after the 20 h OER test.

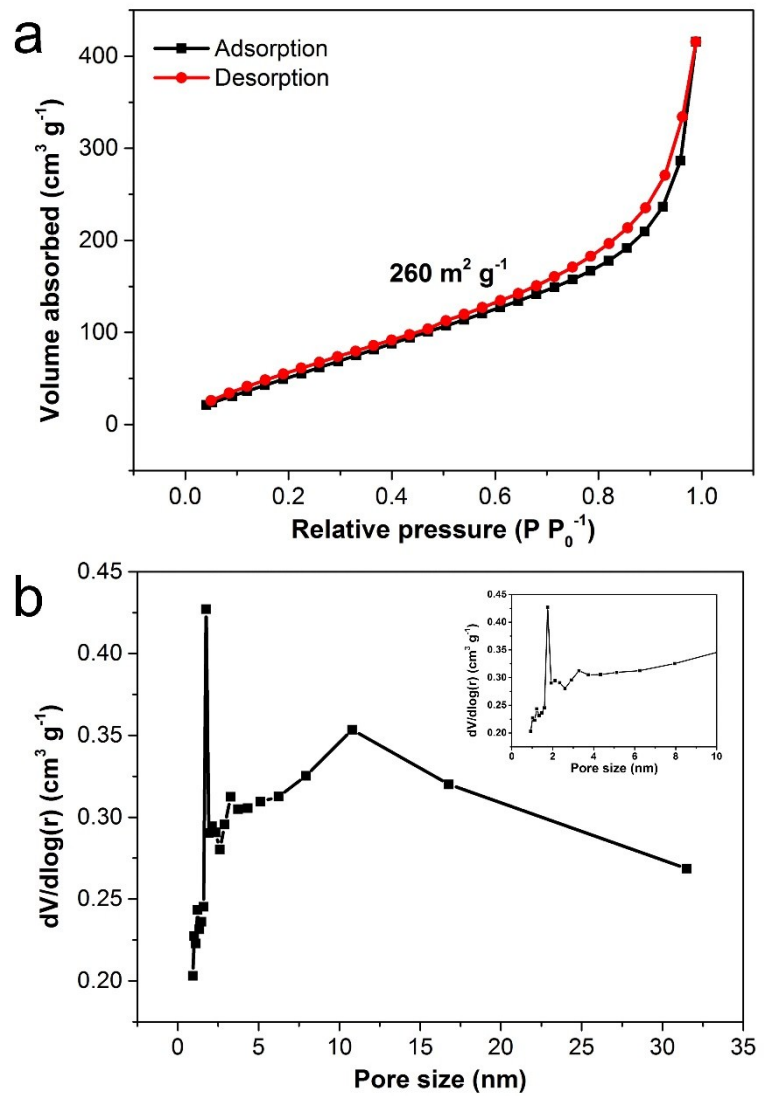


Figure S17. (a) N_2 adsorption-desorption isotherms, and (b) the corresponding BJH pore size distribution of the ultrathin 2D Co-MOF nanosheets (inset: image magnification of pore size distribution from 0 to 10 nm).

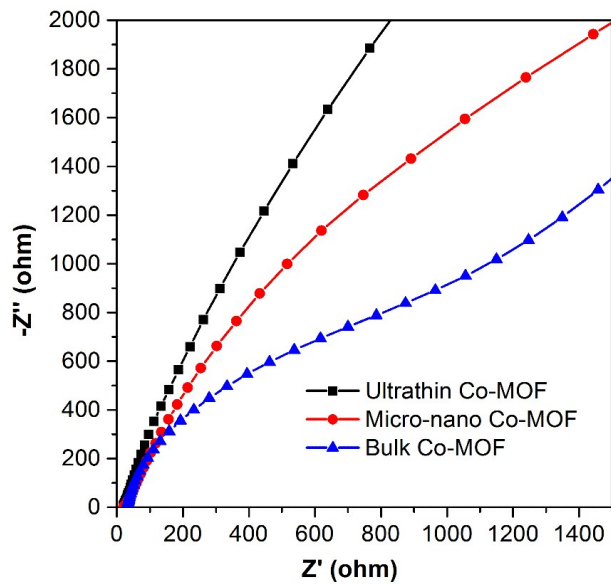


Figure S18. Nyquist plots of the different Co-MOF samples in a frequency range from 100000 to 0.1 Hz.

Table S1. Comparison of the OER activity for several recently reported highly active cobalt-based electrocatalysts and the $\text{Co}_2(\text{OH})_2\text{BDC}$ nanosheets.

Material	Testing condition	$E_{\text{onset}} [\text{V}^{\text{a})}]$	$E_{j=10} [\text{V}^{\text{b})}]$	Tafel slope (mV dec^{-1})	Substrate	Catalyst loading ^{c)}	Ref
MOF(Fe_1-Co_3) _{550N}	0.1 M KOH	1.51	1.62	72.9	GC	0.142	3
Co-CNT/PC	0.1 M KOH	1.49	1.545	73.8	Ni foam	~1	4
Co_3O_4	0.1 M KOH	1.58	1.68	89	GC	~0.35	5
$\text{Co}_3\text{O}_4/\text{N-PC}$	0.1 M KOH	1.52	1.62	72	GC	~0.35	6
Co@NC	0.1 M KOH	1.45	1.69	—	Ni foam	0.21	7
$\text{Co}_3\text{O}_4/\text{C}$ nanowires array	0.1 M KOH	1.47	1.52	70	Cu foil	0.2	8
Co_3O_4	0.1 M KOH	~1.55	1.621	59	GC	0.04	9
Au@ $\text{Co}_3\text{O}_4/\text{C}$	0.1 M KOH	1.53	1.65	60	GC	0.2	9
$\text{Co}_3\text{O}_4/\text{mMWCNT}$	0.1 M KOH	1.51	1.62	—	GC	—	10
$\text{CoSe}_2/\text{Mn}_3\text{O}_4$	0.1 M KOH	1.57	1.68	49	GC	0.2	11
$\text{CoO}_x(4.3)/\text{CNTs}$	0.1 M KOH	1.53	1.62	69	GC	0.15	12
$\text{Co}_{x,y}/\text{NC}$	0.1 M KOH	—	1.66	—	GC	0.21	13
$\text{Ti}_3\text{C}_2\text{T}_x\text{-CoBDC}$	0.1 M KOH	1.51	1.64	48.2	GC	~2.5	14
De-Li CoO_2	0.1 M KOH	—	>1.63	50	GC	~0.1	15
CoP/C	0.1 M KOH	—	1.59	66	GC	~0.05	16
CoP hollow polyhedron	1.0 M KOH	1.53	1.63	57	GC	~0.102	17
Co@ $\text{Co}_3\text{O}_4@\text{NMCC/rGO}$	1.0 M KOH	1.50	1.57	71	GC	~0.298	18
Co P_3 CPs	1.0 M KOH	1.52	1.57	76	Carbon paper	1	19
Co-P film	1.0 M KOH	—	1.575	47	Cu foil	0.19	20
$\text{Co}_{0.5}\text{Fe}_{0.5}\text{S}@/\text{N-MC}$	1.0 M KOH	1.60	1.64	159	GC	0.1	21
UTSA-16	1.0 M KOH	1.60	1.64	77	GC	~0.35	22
Co-MOF	1.0 M KOH	1.65	1.77	125	GC	~0.297	1
Co-MOF@CNTs (5 wt%)	1.0 M KOH	1.51	1.57	69	GC	~0.297	1
Co-MOF/NF	1.0 M KOH	—	—	77	Ni foam	5.84	23
Co(OH)_2	1.0 M KOH	1.542	1.651	95	Carbon cloth	0.2	24
Co_3O_4	1.0 M KOH	1.576	1.675	60	Carbon cloth	0.2	24
CoO_x film	1.0 M KOH	1.53	1.65	42	GC	0.5	25
$\text{CoO}_x@\text{CNT}$	1.0 M KOH	1.56	~1.61	—	GC	~0.42	26
Co(OH)_2	1.0 M NaOH	1.59	1.88	—	FTO glass	3-4	27
Co-NC/CNT	1.0 M KOH	1.51	1.584	78	GC	~0.306	28
$\text{Co}_3\text{O}_4@\text{C-MWCNTs}$	1.0 M KOH	1.50	1.55	62	GC	0.325	2
CoP/rGO-400	1.0 M KOH	1.52	1.57	66	GC	~0.28	29
Co-P/NC	1.0 M KOH	1.55	1.58	52	GC	0.283	30
NiCo-UMOFNs	1.0 M KOH	1.42	1.48	42	GC	0.2	31
CoO/N-doped graphene	1.0 M KOH	1.52	1.57	71	GC	~0.71	32
$\text{Co}_3\text{O}_4/\text{N-rmGO}$	1.0 M KOH	1.50	1.54	67	GC	~0.1	33
CoNi nanosheets	—	1.61	1.68	56.8	GC	—	34
CoMn LDH	1.0 M KOH	—	1.554	43	GC	0.142	35
CoCo LDH	1.0 M KOH	~1.53	1.623	59	GC	0.07	36
NiCo-LDH	1.0 M KOH	1.54	1.597	40	Carbon paper	~0.08	37
$\text{Co}_3\text{O}_4/\text{NiCo}_2\text{O}_4$	1.0 M KOH	1.53	1.57	88	Ni foam	1	38
CoN-1 min	1.0 M KOH	1.50	1.52	70	Ni foam	1.5	39
CoO-MoO ₂ nanocages	1.0 M KOH	1.50	1.542	69	GC	0.5	40
NiCo cages	1.0 M KOH	—	1.61	50	GC	—	41
$\text{CoO}_x\text{-ZIF}$	1.0 M KOH	—	1.548	70.3	GC	—	42
$\text{Co}_2(\text{OH})_2\text{BDC}$ nanosheets	1.0 M KOH	1.411	1.493	74	GC	0.25	This work

^{a)} E_{onset} for onset potential (V vs. RHE); ^{b)} $E_j = 10$ for overpotential required for the current density of 10 mA cm⁻² (V vs. RHE); GC: glassy carbon; ^{c)}Unit: mg cm⁻².

Table S2. Comparison of the OER catalytic performance of different MOFs.

MOF	Onset potential (V vs RHE)	Overpotential at 10 mA cm ⁻² (mV vs RHE)	Tafel slope (mV dec ⁻¹)	TOF at overpotential = 300 mV	Ref
NiCo-UMOFNs	1.42	250	42	0.86 s ⁻¹	31
MOF(Fe ₁ –Co ₃) _{550N}	1.51	390	72.9	0.0033 s ⁻¹ /400 mV	3
NiFe-MOF array	—	240	34	—	43
Fe ₃ -Co ₂ @GC	1.463	283	43	0.27 s ⁻¹	44
Fe/Ni-BTC@NF	—	270	47	0.13 s ⁻¹	45
Fe/Ni _{2.4} /Co _{0.4} -MIL-53	—	219	53.5	—	46
NiPc-MOF	~1.48	350	74	—	47
Cu-MOF	1.39	—	89	—	48
CoCd-MOF	1.583	—	110	0.03314 s ⁻¹	49
Co-MOF/NF	—	311/50 mV cm ⁻²	77	0.18 s ⁻¹ /400 mV	23
UTSA-16	1.60	408	77	—	22
Co₂(OH)₂BDC nanosheets	1.411	273	74	0.23 s⁻¹	This work

References

- 1 Y. Fang, X. Li, F. Li, X. Lin, M. Tian, X. Long, X. An, Y. Fu, J. Jin and J. Ma, *J. Power Sources*, 2016, **326**, 50–59.
- 2 X. Li, Y. Fang, X. Lin, M. Tian, X. An, Y. Fu, R. Li, J. Jin and J. Ma, *J. Mater. Chem. A*, 2015, **3**, 17392–17402.
- 3 Y. Han, J. Zhai, L. Zhang and S. Dong, *Nanoscale*, 2016, **8**, 1033–1039.
- 4 S. Dou, X. Li, L. Tao, J. Huo and S. Wang, *Chem. Commun.*, 2016, **52**, 9727–9730.
- 5 L. Li, T. Tian, J. Jiang and L. Ai, *J. Power Sources*, 2015, **294**, 103–111.
- 6 Y. Hou, J. Li, Z. Wen, S. Cui, C. Yuan and J. Chen, *Nano Energy*, 2015, **12**, 1–8.
- 7 A. Aijaz, J. Masa, C. Rösler, W. Xia, P. Weide, R. A. Fischer, W. Schuhmann and M. Muhler, *ChemElectroChem*, 2017, **4**, 188–193.
- 8 T. Y. Ma, S. Dai, M. Jaroniec and S. Z. Qiao, *J. Am. Chem. Soc.*, 2014, **136**, 13925–13931.
- 9 Z. Zhuang, W. Sheng and Y. Yan, *Adv. Mater.*, 2014, **26**, 3950–3955.
- 10 X. Lu and C. Zhao, *J. Mater. Chem. A*, 2013, **1**, 12053–12059.
- 11 M.-R. Gao, Y.-F. Xu, J. Jiang, Y.-R. Zheng and S.-H. Yu, *J. Am. Chem. Soc.*, 2012, **134**, 2930–2933.
- 12 B. Seo, Y. J. Sa, J. Woo, K. Kwon, J. Park, T. J. Shin, H. Y. Jeong and S. H. Joo, *ACS Catal.*, 2016, **6**, 4347–4355.
- 13 J. Masa, W. Xia, I. Sinev, A. Zhao, Z. Sun, S. Grützke, P. Weide, M. Muhler and W. Schuhmann, *Angew. Chemie Int. Ed.*, 2014, **53**, 8508–8512.
- 14 L. Zhao, B. Dong, S. Li, L. Zhou, L. Lai, Z. Wang, S. Zhao, M. Han, K. Gao, M. Lu, X. Xie, B. Chen, Z. Liu, X. Wang, H. Zhang, H. Li, J. Liu, H. Zhang, X. Huang and W. Huang, *ACS Nano*, 2017, **11**, 5800–5807.
- 15 Z. Lu, H. Wang, D. Kong, K. Yan, P.-C. Hsu, G. Zheng, H. Yao, Z. Liang, X. Sun and Y. Cui, *Nat. Commun.*, 2014, **5**, 1–7.
- 16 B. Seo, Y. J. Sa, J. Woo, K. Kwon, J. Park, T. J. Shin, H. Y. Jeong and S. H. Joo, *ACS Catal.*, 2016, **6**, 4347–4355.
- 17 M. Liu and J. Li, *ACS Appl. Mater. Interfaces*, 2016, **8**, 2158–2165.
- 18 X. Li, Y. Fang, L. Wen, F. Li, G. Yin, W. Chen, X. An, J. Jin and J. Ma, *Dalt. Trans.*, 2016, **45**, 5575–5582.
- 19 T. Wu, M. Pi, X. Wang, D. Zhang and S. Chen, *Phys. Chem. Chem. Phys.*, 2017, **19**, 2104–2110.
- 20 N. Jiang, B. You, M. Sheng and Y. Sun, *Angew. Chemie Int. Ed.*, 2015, **54**, 6251–6254.
- 21 M. Shen, C. Ruan, Y. Chen, C. Jiang, K. Ai and L. Lu, *ACS Appl. Mater. Interfaces*, 2015, **7**, 1207–1218.
- 22 J. Jiang, L. Huang, X. Liu and L. Ai, *ACS Appl. Mater. Interfaces*, 2017, **9**, 7193–7201.
- 23 X. Zhang, W. Sun, H. Du, R.-M. Kong and F. Qu, *Inorg. Chem. Front.*, 2018, **5**, 344–347.
- 24 X.-F. Lu, P.-Q. Liao, J.-W. Wang, J.-X. Wu, X.-W. Chen, C.-T. He, J.-P. Zhang, G.-R. Li and X.-M. Chen, *J. Am. Chem. Soc.*, 2016, **138**, 8336–8339.
- 25 L. Trotochaud, J. K. Ranney, K. N. Williams and S. W. Boettcher, *J. Am. Chem. Soc.*, 2012, **134**, 17253–17261.
- 26 H. Jin, J. Wang, D. Su, Z. Wei, Z. Pang and Y. Wang, *J. Am. Chem. Soc.*, 2015, **137**, 2688–2694.
- 27 Y. Zhang, B. Cui, O. Derr, Z. Yao, Z. Qin, X. Deng, J. Li and H. Lin, *Nanoscale*, 2014, **6**, 3376–3383.
- 28 X. Li, Y. Fang, X. Lin, M. Tian, X. An, Y. Fu, R. Li, J. Jin and J. Ma, *J. Mater. Chem. A*, 2015, **3**, 17392–17402.
- 29 L. Jiao, Y.-X. Zhou and H.-L. Jiang, *Chem. Sci.*, 2016, **7**, 1690–1695.
- 30 B. You, N. Jiang, M. Sheng, S. Gul, J. Yano and Y. Sun, *Chem. Mater.*, 2015, **27**, 7636–7642.
- 31 S. Zhao, Y. Wang, J. Dong, C.-T. He, H. Yin, P. An, K. Zhao, X. Zhang, C. Gao, L. Zhang, J. Lv, J. Wang, J. Zhang, A. M. Khattak, N. A. Khan, Z. Wei, J. Zhang, S. Liu, H. Zhao and Z. Tang, *Nat. Energy*, 2016, **1**, 16184.
- 32 S. Mao, Z. Wen, T. Huang, Y. Hou and J. Chen, *Energy Environ. Sci.*, 2014, **7**, 609–616.
- 33 Y. Liang, Y. Li, H. Wang, J. Zhou, J. Wang, T. Regier and H. Dai, *Nat. Mater.*, 2011, **10**, 780–786.
- 34 B. Ni and X. Wang, *Chem. Sci.*, 2015, **6**, 3572–3576.
- 35 F. Song and X. Hu, *J. Am. Chem. Soc.*, 2014, **136**, 16481–16484.

- 36 F. Song and X. Hu, *Nat. Commun.*, 2014, **5**, 1–9.
- 37 H. Liang, F. Meng, M. Cabán-Acevedo, L. Li, A. Forticaux, L. Xiu, Z. Wang and S. Jin, *Nano Lett.*, 2015, **15**, 1421–1427.
- 38 H. Hu, B. Guan, B. Xia and X. W. (David) Lou, *J. Am. Chem. Soc.*, 2015, **137**, 5590–5595.
- 39 Y. Zhang, B. Ouyang, J. Xu, G. Jia, S. Chen, R. S. Rawat and H. J. Fan, *Angew. Chemie*, 2016, **128**, 1–6.
- 40 F. Lyu, Y. Bai, Z. Li, W. Xu, Q. Wang, J. Mao, L. Wang, X. Zhang and Y. Yin, *Adv. Funct. Mater.*, 2017, **27**, 1702324.
- 41 L. Han, X.-Y. Yu and X. W. (David) Lou, *Adv. Mater.*, 2016, **28**, 4601–4605.
- 42 S. Dou, C.-L. Dong, Z. Hu, Y.-C. Huang, J. Chen, L. Tao, D. Yan, D. Chen, S. Shen, S. Chou and S. Wang, *Adv. Funct. Mater.*, 2017, **27**, 1702546.
- 43 J. Duan, S. Chen and C. Zhao, *Nat. Commun.*, 2017, **8**, 15341.
- 44 J.-Q. Shen, P.-Q. Liao, D.-D. Zhou, C.-T. He, J.-X. Wu, W.-X. Zhang, J.-P. Zhang and X.-M. Chen, *J. Am. Chem. Soc.*, 2017, **139**, 1778–1781.
- 45 L. Wang, Y. Wu, R. Cao, L. Ren, M. Chen, X. Feng, J. Zhou and B. Wang, *ACS Appl. Mater. Interfaces*, 2016, **8**, 16736–16743.
- 46 F.-L. Li, Q. Shao, X. Huang and J.-P. Lang, *Angew. Chemie Int. Ed.*, 2017, 1–6.
- 47 H. Jia, Y. Yao, J. Zhao, Y. Gao, Z. Luo and P. Du, *J. Mater. Chem. A*, 2018, **6**, 1188–1195.
- 48 M. Jahan, Z. Liu and K. P. Loh, *Adv. Funct. Mater.*, 2013, **23**, 5363–5372.
- 49 K. Maity, K. Bhunia, D. Pradhan and K. Biradha, *ACS Appl. Mater. Interfaces*, 2017, **9**, 37548–37553.